

# Bauxite ‘red mud’ in the ceramic industry. Part 2: production of clay-based ceramics

Vincenzo M. Sglavo<sup>a,\*</sup>, Stefano Maurina<sup>a</sup>, Alexia Conci<sup>a</sup>, Antonio Salviati<sup>a</sup>,  
Giovanni Carturan<sup>a</sup>, Giorgio Cocco<sup>b</sup>

<sup>a</sup>*Dipartimento di Ingegneria dei Materiali, Università di Trento, Via Mesiano 77, I-38050 Trento, Italy*

<sup>b</sup>*Dipartimento di Chimica Fisica, Università di Sassari, Via Vienna 2, I-07100 Sassari, Italy*

Received 4 February 1999; received in revised form 1 April 1999; accepted 11 May 1999

---

## Abstract

Some potential uses of red mud as a raw component in clay mixtures for ceramic bodies production are presented. The influence of increasing amounts of red mud on the forming procedure, sintering and final properties was analyzed. Samples were produced by uniaxial pressing and slip casting. Two different clays are used as basic materials, the former being currently employed for the production of bricks by extrusion, the second — almost pure Kaolin — for high quality ceramic manufacturing. In both cases the addition of red mud led to more deflocculated solid–water systems and an increase of the critical moisture content. Mixtures prepared with the first clay and red mud loads up to 50% were fired at 850°C. The red mud content did not influence the sample porosity while determining a strength decrease attributed to the inertness of red mud at the working temperature. Samples produced using the second clay and red mud (0–20%) were fired at 950 and 1050°C. The addition of red mud determined increases of density and flexural strength which can be accounted for by the formation of a larger amount of glassy phase at higher red mud contents. The results of this work indicate excellent perspectives for using ‘red mud’ as raw material in mixtures with clay for the production of ceramic bodies. © 2000 Elsevier Science Ltd. All rights reserved.

*Keywords:* Clays; Red mud; Sintering; Mechanical properties; Porosity; Bauxite

---

## 1. Introduction

The enormous quantity of ‘red mud’ discharged by industries producing alumina from bauxite represents an environmental and economical problem. Numerous reports proposing re-uses of ‘red mud’ have been advanced, especially for the production of ceramic bodies or cements.<sup>1–11</sup> Along this line of research, a deep characterization of the red mud has been presented in a companion paper, hereafter Part 1.<sup>12</sup> Special attention has been paid to the structural transformations and cross-reactions induced by heating representative batches of red mud up to 1400°C. A full knowledge of the thermal behaviour seemed to us of prior concern for possible applications requiring mixing with other raw materials and firing at different temperatures.

Dried red mud was substantially inert up to 900°C, the loss of H<sub>2</sub>O from aluminium hydroxides and of CO<sub>2</sub> from silico-alumino-carbonates being the only detectable effects. Between 900 and 1100°C complementary reactions occurred, yielding Ca<sub>3</sub>Al<sub>2</sub>O<sub>6</sub>, NaAlSiO<sub>4</sub> and Na<sub>2</sub>SiO<sub>5</sub>. Concurrent with the melting of nepheline-like compounds, the colour turned from orange-red to dark red. At higher temperatures major components such as Fe<sub>2</sub>O<sub>3</sub> and TiO<sub>2</sub> reacted to give Fe<sub>2</sub>TiO<sub>4</sub> with O<sub>2</sub> evolution. This reaction was responsible for the intensification of the brown colour above 1200°C.<sup>12</sup>

These results were used as guidelines to test the red mud as a raw component in clay mixtures for the production of ceramic bodies. In this work we report on the influence of the red mud on the forming procedure, strength, porosity and colour of conventional clay-based products obtained with different processing techniques. Two different clays were considered. The first one (A) is industrially used for the production of bricks and it is commonly mixed with a less valuable clay producing a plastic paste upon addition of ≈25% of water. The

---

\* Corresponding author. Tel.: +39-0461-882468; fax: +39-0461-881977.

*E-mail address:* sglavo@ing.unitn.it (V.M. Sglavo).

paste is extruded for the formation of the green body which is fired at 850°C. The obtained bricks show a characteristic orange — red colour. The second high quality clay (B) is used for the production of sanitary-ware by slip casting. The resulting products, sintered at 1200°C, display a perfectly white coloration.

The production of ceramic compacts containing different amounts of red mud was performed with a double objective. The use of red mud in mixtures with clay A was addressed to a partial substitution of ordinary clay for production of bricks still maintaining the current industrial procedures. The study of ceramic compacts produced from red mud and clay B aimed at defining the influence of red mud on sintering and final properties of ceramic bodies produced from Kaolin.

## 2. Experimental procedure

The red mud was obtained from Eurallumina (Porto Vesme, Cagliari, Italy) and dried at 120°C for 2 h. The two different clays, labelled as A (Fornaci Scanu, Sestu, Cagliari, Italy) and B (ECC International Europe, Cornwall, England), were milled into powders with particles size lower than 100 µm and characterized by X-ray diffraction (D/MAX, Rigaku, Japan) and by thermogravimetric and thermodifferential analyses (STA 409, Netzsch, Germany). The chemical composition was determined by X-ray fluorescence analysis (X' Unique 11, Philips, The Netherlands).

Clay A was mixed with different amounts of red mud ranging from 0 to 50% of the solid weight. Water was added to the powder mixtures to obtain a plastic mass which was used to produce hand-made cylindrical samples (length ≈ 40 mm, diameter ≈ 5 mm). These specimens were dried for intervals of about 1 min at 100–120°C monitoring their weight and length changes. This allowed the determination of the shrinkage,  $\Delta l/l_0$ , as a function of the moisture content,  $H$ .  $\Delta l/l_0$  was calculated as the elongation with respect to fully dried sample,  $H$  with reference to the solid mass.

Circular samples (diameter = 35 mm, thickness = 4–5 mm) were obtained by uniaxial pressing of red mud/clay A/water mixtures using a maximum pressure of 10 MPa. The plasticity of the samples was evaluated from the penetration at different applied loads of a steel sphere (diameter = 15 mm) into the green body. A suitable amount of water was employed in these samples to reproduce a plastic behaviour similar to that of the green compacts currently produced by Fornaci Scanu.

Another set of samples was produced by slip casting. Slip containing equal amounts of water and solid was poured into Plaster of Paris moulds which allowed the preparation of circular samples (diameter = 35 mm).

Green samples produced by pressing and slip casting were sintered in air for 15 min at 850°C which represents

the maximum temperature used in the brick production plants (Fornaci Scanu).

Clay B was loaded with red mud amounts ranging from 0 to 20% of the solid weight. The shrinkage upon drying was studied as described previously for clay A-red mud mixtures.

Circular samples were produced by uniaxial pressing and by slip casting according to the procedures described before. An amount of 5 wt% of water was used in this case. Green specimens were fired at 950 and 1050°C for 15 min, these two temperatures being chosen owing to important thermal evolutions observed by preliminary thermal analyses.

Specimens porosity was measured by mercury porosimetry (Carlo Erba, Model 2000, Italy). The density was calculated from the weight/volume ratio. Crystal-line phases evolution was studied by X-ray diffraction (XRD) analysis on sintered specimens.

Mechanical strength was measured using a universal mechanical testing machine (MTS System, Model 810, USA) by biaxial flexure using the piston on three balls procedure.<sup>13</sup> Tests were performed using a distance between balls of 25 mm and a piston of 1 mm diameter. Due to the irregular shape of the specimens produced by slip casting, these were initially reduced to regular disk geometry using SiC paper. The surfaces of all specimens were polished with silicon carbide paper (1000 grid) prior to mechanical testing.

## 3. Results and discussion

### 3.1. Thermal behaviour of clays

The chemical compositions of clays A and B are shown in Table 1. Table 2 reports the main phases detected by X-ray diffraction analysis.

Fig. 1 shows the thermogravimetric (TG) and thermodifferential (DT) plots of clays A and B. DT diagram for clay A shows an endothermic peak at about 120°C, attributed to adsorbed water evaporation.<sup>14</sup> Small endothermic signals at around 530°C corresponds to H<sub>2</sub>O loss from Illite, affording meta-Kaolin.<sup>15,16</sup> The deep peak at 840°C, corresponding to the decomposition of CaCO<sub>3</sub>, is associated to the ≈ 15% weight loss observed in the TG curve, in agreement with the CaCO<sub>3</sub> content of clay A.<sup>16</sup> The availability of reactive CaO at 850°C promotes the formation of Gehlenite (Ca<sub>2</sub>Al<sub>2</sub>SiO<sub>7</sub>) for reaction with meta-Kaolin; as indicated by XRD analysis, the involvement of both Quartz and Anorthoclase is excluded, these phases being inert at this temperature. The heat absorption detected at 1190°C is attributed to the crystallization of Mullite from meta-Kaolin.<sup>15–19</sup>

The thermal analysis of clay B shows a fundamental weight loss at 530°C associated to a definite endothermic

Table 1  
Chemical composition (wt%) of clay A and B (LOI = loss on ignition at 900°C)

	SiO <sub>2</sub>	Al <sub>2</sub> O <sub>3</sub>	K <sub>2</sub> O	Na <sub>2</sub> O	TiO <sub>2</sub>	CaO	Fe <sub>2</sub> O <sub>3</sub>	LOI	other
A	37.5	10.8	2.0	0.9	0.6	22.1	4.1	18.7	3.3
B	52.9	28.4	2.0	0.1	1.1	0.2	1.2	13.4	0.7

Table 2  
Crystallographic phases detected in clay A and B

	Major constituents	Minor constituents
A	Calcite (CaCO <sub>3</sub> ) Quartz (SiO <sub>2</sub> )	Illite ((K <sub>2</sub> ,Mg)Al <sub>2</sub> Si <sub>3</sub> O <sub>10</sub> (OH) <sub>2</sub> ) Anorthoclase ((Na,K)AlSi <sub>3</sub> O <sub>8</sub> )
B	Kaolin (Al <sub>2</sub> Si <sub>2</sub> O <sub>7</sub> (OH) <sub>4</sub> ) Quartz (SiO <sub>2</sub> )	Lizardite ((MgAl) <sub>3</sub> (SiAl) <sub>2</sub> O <sub>5</sub> (OH) <sub>4</sub> ) Brammallite (NaAl <sub>2</sub> (SiAl) <sub>4</sub> O <sub>10</sub> (OH) <sub>2</sub> )

peak, suggesting the decomposition of Kaolin, Lizardite and Brammallite into water and meta-kaolin.<sup>\*15–19</sup> The evident kaolinite, Lizardite and Brammallite into water and meta-Kaolin. exothermic effect at 990°C is attributed to the transformation of meta-Kaolin into Mullite. This process is accompanied by the formation of a relatively abundant glassy phase, revealed by X-ray diffraction analysis as a broad band centered at diffraction angles around 20°. This transformation prompted us to select 950°C and 1050°C for sintering of green bodies produced using clay B. The exothermic effect at 1365°C is attributed to crystallization of Mullite from residual meta-Kaolin and Quartz, the process requiring a further segregation of glassy phase as indicated by valuable increase of the corresponding broad band at ≈20°.<sup>17,18</sup>

### 3.2. Forming and drying behaviour

The correlation between water content, shrinkage effects and mixture compositions are shown in Fig. 2. In the case of red mud + clay A [Fig. 2(a)], the  $H$  vs  $\Delta l/l_0$  trends show an upward shift as the red mud content increases. Likewise, the leather-hard moisture content, also referred to as the critical moisture content,<sup>17</sup> increases from ≈ 14 to ≈ 27% as the percentage of red mud varies from 0 to 50%. This behaviour may be related to residual NaOH in the red mud,<sup>1–3,5,12</sup> which determines a basic pH of the suspension, ultimately promoting a more deflocculated suspension with larger amounts of interstitial water.<sup>14–17,20</sup> The finer red mud grain size<sup>12</sup> can also account for the higher critical moisture content observed in Fig. 2(a).<sup>14–17</sup>

\* In some papers, the phase 2Al<sub>2</sub>O<sub>3</sub>·SiO<sub>2</sub>, is identified as pseudo-Mullite<sup>17</sup> or Spinel<sup>18</sup>.

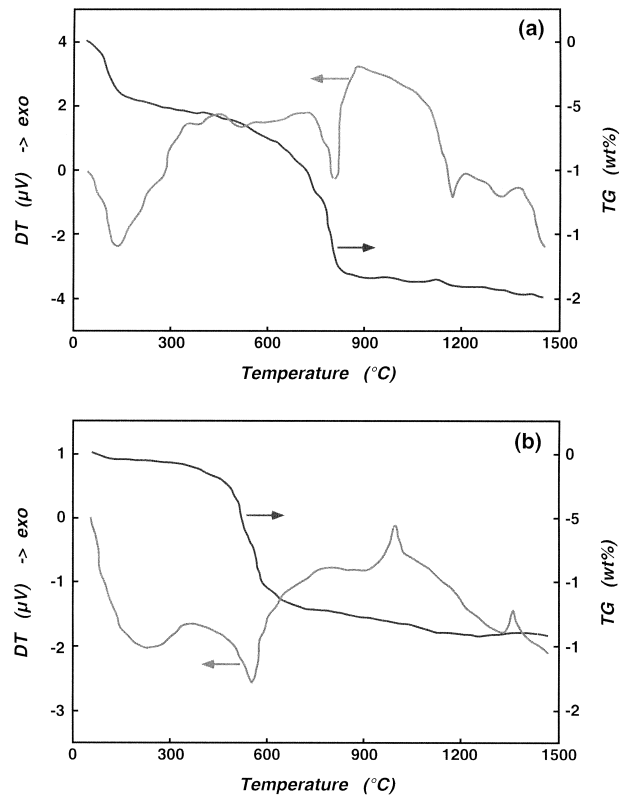


Fig. 1. Thermogravimetric (TG) and differential thermal (DT) diagram of clay (a) A and (b) B.

For the sake of comparison, the red mud/clay mixtures showing a plasticity similar to that of the formulation currently used in the brick production by extrusion are evidenced as large full circles in Fig. 2(a). For pure clay A, this value was obtained in presence of 22 wt% of water. In the case of red mud mixtures, higher water contents are required to reach the same plastic behaviour, but with an important decrease of  $\Delta l/l_0$  which is of about 1% for the 50% red mud/clay A mixture. Indeed smaller shrinkage of the green compact are observed upon drying<sup>14–17,20</sup> owing to the suspension deflocculation induced by the red mud alkali content. These results are important from a technological point of view as higher heating rates upon drying are allowed with possible production of compacts with larger dimensions.

Fig. 2(b) shows the shrinkage behaviour for humid bodies produced with clay B (almost pure Quartz and Kaolin). The  $H$  vs  $\Delta l/l_0$  trends are shifted upward even for small additions of red mud, a stationary condition being reached with minor red mud percentages. In this case, the leather-hard moisture content rises from ≈ 14 to ≈ 20% for a red mud addition of 1%. This fact can again be related to clay suspension deflocculation promoted by the alkaline contamination of red mud. It was observed that red mud loads as small as 1% determine water-clay mixture pH values higher than 7–8,

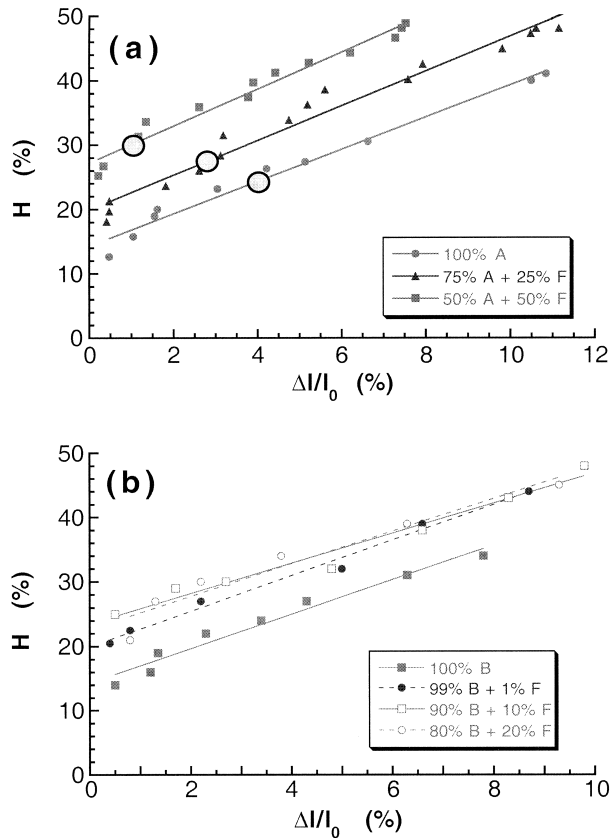


Fig. 2. Plot of  $H$  as a function of  $\Delta l/l_0$  for clay (a) A and (b) B.  $F$  represents red mud content. Large dashed circles correspond to system compositions with plasticity similar to that of the formulation used in brick production (Fornaci Seanu).

thus promoting a fully stabilized suspension.<sup>18,20</sup> In these conditions, both Quartz and Kaolin grains surfaces are negatively charged as pH is higher than the corresponding isoelectric point.<sup>20</sup>

### 3.3. Properties of fired ceramics

Ceramics compacts prepared by pressing and slip casting of clay A and red mud mixtures were fired at 850°C. Density, porosity and average pore radius values are collected in Fig. 3 as a function of the red mud percentage. It appears that the amount of red mud and the processing procedure are of slight consequence for the quoted quantities. Density remains constant, around 1.5 g/cm<sup>3</sup>, in spite of red mud specific density ( $\approx 5.3$  g/cm<sup>3</sup>)<sup>12</sup> which is sensibly higher than clay density ( $\approx 3.3$  g/cm<sup>3</sup>). Similarly, porosity and pore radius are independent on red mud content. This effect can be related to the suspension stabilization promoted by red mud addition which determines deflocculation and, consequently, a more open particle packing. Nevertheless, due to the extreme dispersion of red mud particles (diameter  $\approx 0.1$   $\mu\text{m}$ ), partial filling of interstices among clay particles can be envisaged. Compact porosity may also be

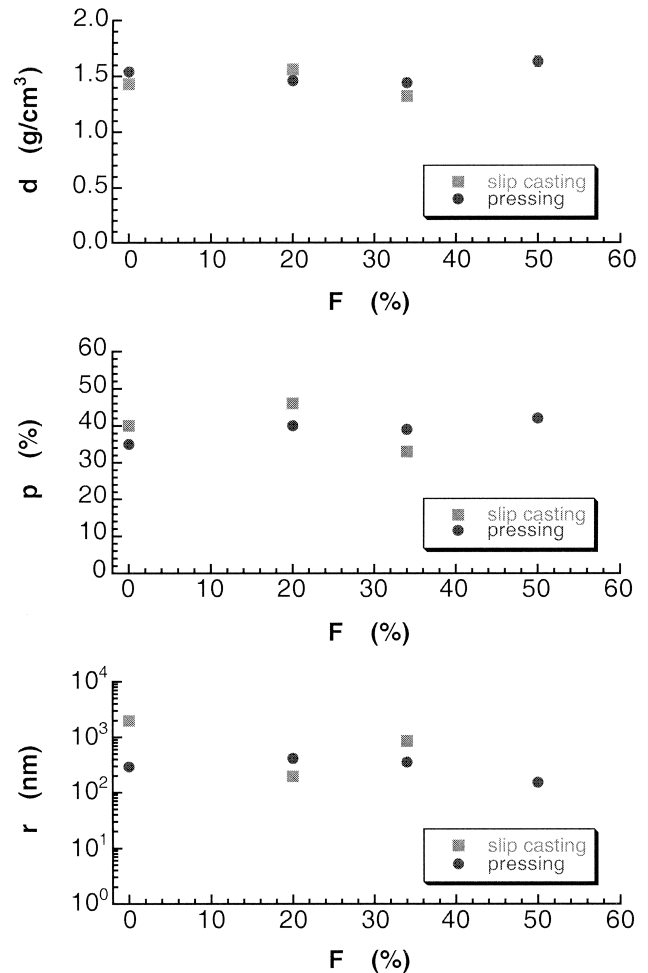


Fig. 3. Density ( $d$ ), porosity ( $p$ ) and average pore radius ( $r$ ) for clay A - based compacts.  $F$  represents red mud content.

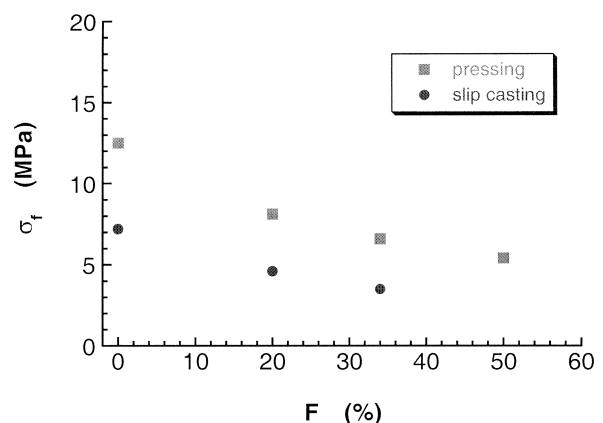


Fig. 4. Flexural strength ( $\sigma_f$ ) for clay A - based compacts.  $F$  represents red mud content.

affected by the presence of CaCO<sub>3</sub> in clay A (about 40%): porosity arising from carbonate decomposition to CaO and CO<sub>2</sub> can compensate the pore filling due to higher dispersion of red mud.

Table 3  
Crystallographic and glass phases in fired samples

Composition	Firing temperature	Major constituents	Minor constituents
100% clay A	850°C	Quartz (SiO <sub>2</sub> ) Gehlenite (Ca <sub>2</sub> Al <sub>2</sub> SiO <sub>7</sub> )	Illite ((K <sub>2</sub> ,Mg)Al <sub>2</sub> Si <sub>3</sub> O <sub>10</sub> (OH) <sub>2</sub> ) Anorthoclase ((Na,K)AlSi <sub>3</sub> O <sub>8</sub> )
50% clay A + 50% red mud	850°C	Quartz (SiO <sub>2</sub> ) Gehlenite (Ca <sub>2</sub> Al <sub>2</sub> SiO <sub>7</sub> ) Hematite (Fe <sub>2</sub> O <sub>3</sub> )	Illite ((K <sub>2</sub> ,Mg)Al <sub>2</sub> Si <sub>3</sub> O <sub>10</sub> (OH) <sub>2</sub> ) Anorthoclase ((Na,K)AlSi <sub>3</sub> O <sub>8</sub> ) Ca <sub>3</sub> Al <sub>2</sub> O <sub>6</sub>
100% clay B	950°C	Quartz (SiO <sub>2</sub> ) Silicate glass phase	Meta-kaolin Mullite (3(Al <sub>2</sub> O <sub>3</sub> ) <sub>2</sub> SiO <sub>2</sub> )
	1050°C	Quartz (SiO <sub>2</sub> ) Mullite (3(Al <sub>2</sub> O <sub>3</sub> ) <sub>2</sub> SiO <sub>2</sub> ) Silicate glass phase	Meta-kaolin
80% clay B + 20% red mud	950°C	Quartz (SiO <sub>2</sub> ) Hematite (Fe <sub>2</sub> O <sub>3</sub> ) Silicate glass phase	Meta-kaolin Ca <sub>3</sub> Al <sub>2</sub> O <sub>6</sub>
	1050°C	Quartz (SiO <sub>2</sub> ) Hematite (Fe <sub>2</sub> O <sub>3</sub> ) Mullite (3(Al <sub>2</sub> O <sub>3</sub> ) <sub>2</sub> SiO <sub>2</sub> ) Silicate glass phase	Meta-kaolin Ca <sub>3</sub> Al <sub>2</sub> O <sub>6</sub>

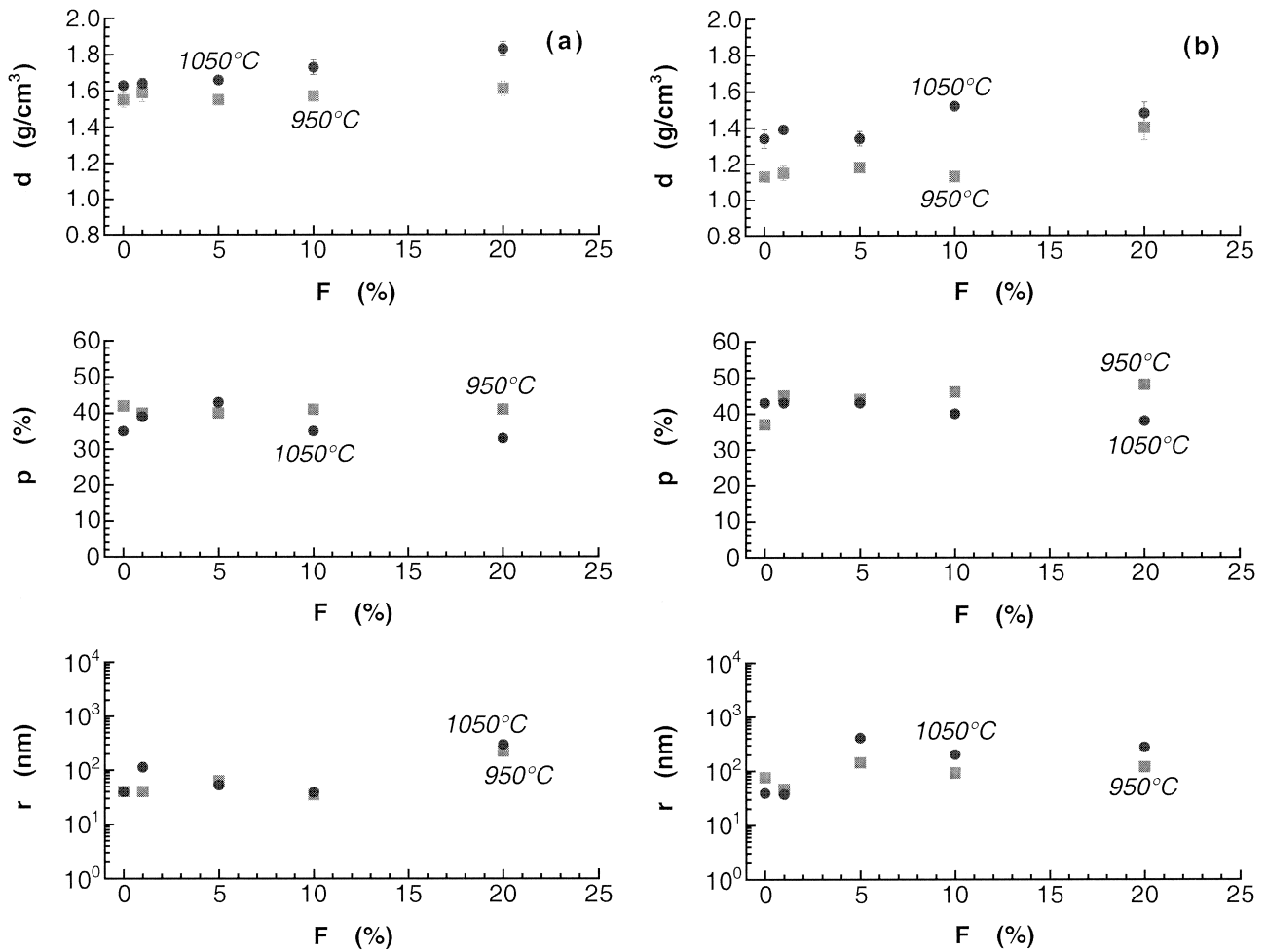


Fig. 5. Density ( $d$ ), porosity ( $p$ ) and average pore radius ( $r$ ) for clay B - based compacts produced by (a) uniaxial pressing and (b) slip casting.  $F$  represents red mud content.

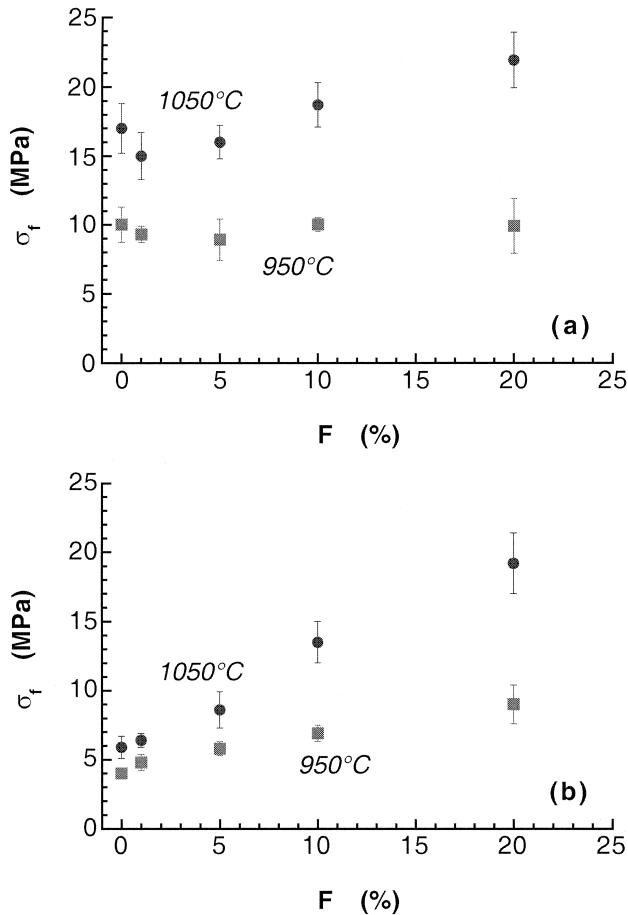


Fig. 6. Flexural strength ( $\sigma_f$ ) for clay B - based compacts produced by (a) uniaxial pressing and (b) slip casting.  $F$  represents red mud content.

The mechanical strength of samples produced at 850°C from clay A is plotted in Fig. 4. Higher red mud loads determine lower strength according to the inertness of the red mud at this temperature. As a matter of fact, X-ray diffraction analysis on fired mixtures shows the same evolution of crystalline phases observed in pure clay A (Table 3, where CaO from Calcite decomposition reacts with meta-Kaolin to produce Gehlenite ( $\text{Ca}_2\text{Al}_2\text{SiO}_7$ ) which, at 850°C, mainly determines the mechanical strength of the ceramic body. The addition of red mud to clay A does not change the oxide mass involved in this reaction with minor formation of  $\text{Ca}_3\text{Al}_2\text{O}_6$  contributing to the strength of compacts at the highest red mud percentages.

Mechanical properties are also affected by the processing procedure. As shown in Fig. 4, failure stress is sensibly smaller ( $\approx 50\%$  less) for samples produced by slip casting. Since samples produced by slip casting or pressing display a similar porosity,  $\sigma_f$  data may properly be related to the texture of the resulting matrix. The application of an external force during uniaxial pressing

can determine a favourable rearrangement of the clay particles, irrespectively of the finite electrical double layer, with a valuable increase of contact points. Conversely, during slip casting, the well deflocculated suspension does not evolve to a fully packed body.

Density, porosity and average pore radius of samples produced from red mud and clay B at 950 and 1050°C are shown in Fig. 5(a) (pressing) and Fig. 5(b) (slip casting). Strength values are reported in Fig. 6(a) and (b), respectively. Regardless of red mud load, firing temperature and processing procedure, porosity and average pore radius remain constant. Conversely, as the red mud content is increased, valuable increases of density and failure stress are observed particularly for samples produced by uniaxial pressing and fired at 1050°C. Because the external force can overcome the repulsion potential determined by the electrical double layer, higher density values are expected owing to the high red mud density. Accordingly,  $\sigma_f$  values are proportional to the red mud content and firing temperature, especially for samples obtained by uniaxial pressing.

The evolution of density, porosity and failure stress of these compacts can be related to the phase and texture transformation upon firing. X-ray diffraction analyses performed on clay B fired at 950°C (Table 3) revealed the decomposition of Kaolin into meta-Kaolin and the formation of a glassy phase with limited consumption of Quartz. Furthermore, crystallization of Mullite and formation of larger amounts of silicate glass were observed at 1050°C. These transformations account for the higher strength and density measured at 1050°C. Crossed reactions between clay B and red mud can also be pointed out on the basis of XRD analysis. At 950 and 1050°C the intensity of the XRD broad signal corresponding to glassy phase increases with the red mud content. This fact suggests that Nepheline ( $\text{NaAlSi}_3\text{O}_8$ ) and sodium silicate ( $\alpha\text{-Na}_2\text{Si}_2\text{O}_5$ ), already present in the red mud heated above 900°C,<sup>12</sup> participate to the glassy phase, this effect being more pronounced as firing temperature increases. Indeed, no crystalline Nepheline or sodium silicate were detected by XRD in such samples. Further strength increase can be related to the formation of  $\text{Ca}_3\text{Al}_2\text{O}_6$  in red mud. These crossed reactions between clay B and red mud can explain the different trend shown by  $\sigma_f$  as a function of the processing procedure. In addition, the higher temperatures used for sintering clay B-based products limit the effect of the deflocculation promoted by red mud addition previously discussed.

From a technological point of view, proposed arguments point out that failure strength of samples produced from clay B increases with red mud load, the phenomenon being more pronounced at higher firing temperatures. In addition, the formation of glassy phase, especially at 1050°C, can account for the limited porosity decrease as red mud load increases (Fig. 5).

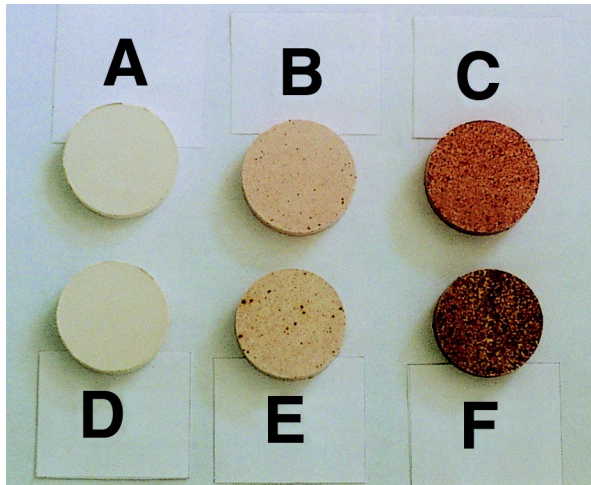


Fig. 7. Specimens produced by pressing using clay B. Fired at 950°C: A (0% red mud), B (5% red mud), C (20% red mud). Fired at 1050°C: D (0% red mud), E (5% red mud), F (20% red mud).

Clay B + red mud specimens produced by pressing are shown in Fig. 7. The chromatic evolution as a function of red mud content and firing temperature deserves some comments. At 950°C, the white colour of pure clay turns pink in the presence of 20% red mud. At 1050°C, the fundamental tone is violet, whose intensity depends on the amount of red mud. These facets suggest a possible exploitation of red mud as versatile colorant for ceramic materials.

#### 4. Conclusions

The results of this work point out the possibility of using 'red mud' as raw material in mixtures with clay for the production of ceramic bodies. Red mud influences both forming procedures and final properties of fired materials. Due to alkaline contamination, red mud is responsible for a more deflocculated suspension resulting in a higher leather-hard moisture content. These qualities are important from a technological point of view since this allows the production of green bodies with smaller shrinkage upon drying. Below 900°C, red mud can be considered an inert component in mixtures with carbonate-rich clays so that the mechanical strength decreases as the red mud concentration increases. Conversely, red mud represents a reactive phase above 950–1000°C, promoting higher strength in mixtures with Kaolin. In addition to this, red mud represents a low cost colorant for ceramic materials as orange-red and pink-violet gradations can be obtained in mixtures with white clays sintered below and above 1000°C, respectively.

#### Acknowledgements

This work was supported by EMSA (Cagliari, Italy) under Contract EMSA-INCM 'Riutilizzo di fanghi rossi'. Dr. Ullu (EMSA, Cagliari, Italy), Dr. Teodosi (Eurallumina, Porto Vesme, Cagliari, Italy) and Ing. G. Scanu (Fornaci Scanu, Cagliari, Italy) are acknowledged for their collaboration.

#### References

1. Bayer, G., Möglichkeiten zur Wirtschaftlichen Beseitigung von Rotschlamm. *Erzmetall.*, 1972, **25**(9), 454–457 (in German).
2. Parek, B. K. and Goldberger, W., An assessment of technology for possible utilization of Bayer process muds. Battelle Columbus Labs Report no. EPA60012-76-301, Columbus, OH, USA, 1976.
3. Di San Filippo, A., Riutilizzo del Fango Rosso. *Rendiconti del Seminario della Facoltà di Scienze dell'Università di Cagliari*, Vol. L [3–4], Sigla Esse, Cagliari (Italy), 1980 (in Italian).
4. Haake, G., Rotschlamm-Abfall oder Verwertbares Nebenprodukt? *Neue Hutte*, 1988, **33**(11), 424–429 (in German).
5. Musselman, L. L., Production processes, properties and applications for aluminum-containing hydroxides. In *Alumina Chemicals: Science and Technology Handbook*, ed. L. D. Hart. The American Ceramic Society, Columbus, OH, USA, 1990, pp. 75–92.
6. Lotze, J. and Wargalla, G., Rotschlamm-Ein Baustoff zur Deponie-Basisabdichtung. *Erzmetall.*, 1986, **39**(7–8), 394–398 (in German).
7. Tauber, T., Hill, R. K., Crook, D. N. and Murray, M. J., Red mud residues from alumina production as a raw material for heavy clay products. *J. Austr. Ceram. Soc.*, 1971, **7**(1), 12–17.
8. Knight, J. C., Wagh, A. S. and Reid, W. A., The mechanical properties of ceramics from bauxite waste. *J. Mater. Sci.*, 1986, **21**, 2179–2184.
9. Wagh, A. S. and Douse, V. E., Silicate bonded unsintered ceramics of Bayer process waste. *J. Mater. Res.*, 1991, **6**(5), 1094–1102.
10. Wagh, A. S. and Douse, V. E., Silicate bonding of laterites — an ancient process for construction components. In *Ceramics and Civilization, Vol. VI, The Social and Cultural Contexts of New Ceramic Technologies*, ed. W. D. Kingery. The American Ceramic Society, Westerville, OH, USA, 1993, pp. 75–87.
11. Kara, M., Emrullahoglu, Ö.F., Study of Seydisehir red mud wastes as brick and roofing tiles. In *Fourth Euroceramics, Vol. 12*, ed. I. Braga, S. Cavallini and G. F. Di Cesare. Faenza Editrice, Faenza, Italy, 1995, pp. 155–162.
12. Sglavo, V. M., Campostrini, R., Maurina, S., Carturan, G., Monagheddu, M., Budroni, G. and Cocco, G., Bauxite 'Red Mud' in the ceramic industry. Part I. thermal behaviour. *J. Eur. Ceram. Soc.*
13. Shetty, D. K., Rosenfield, A. R., McGuire, P., Bansal, G. K. and Duckworth, W. H., Biaxial flexure tests for ceramics. *Ceramic Bull.*, 1980, **59**(12), 1193–1197.
14. Ford, R. W., *Ceramics Drying*. Pergamon Press, Oxford, UK, 1986.
15. Worrall, W. E., *Ceramic Raw Materials*. Pergamon Press, Oxford, UK, 1982.
16. Ravaglioli, A., Fiori, C. and Fabbri, B., *Materie Prime Ceramiche Vol. 3*. Faenza Editrice, Faenza, Italy, 1989 (in Italian).
17. Worrall, W. E., *Clays and Ceramic Raw Materials, 2nd edn*. Elsevier Applied Science Publishers, London, UK, 1986.

18. Aksay, I. A., Dabbs, D. M. and Sarikaya, M., Mullite for structural, electronic, and optical applications. *J. Am. Ceram. Soc.*, 1991, **74**(10), 2343–2358.
19. Pask, J. A. and Tompkins, A. P., Formation of mullite from sol-gel mixtures and kaolinite. *J. Am. Ceram. Soc.*, 1991, **74**(10), 2367–2373.
20. Reed, J. S., *Principles of Ceramics Processing*, 2nd edn. J. Wiley and Sons, New York, USA, 1995.